

Sex specific inflammatory profiles of cerebellar mitochondria are attenuated in Parkinson's disease

Thomas L. Ingram¹, Freya Shephard¹, Sarir Sarmad², Catherine A. Ortori², David A. Barrett², Lisa Chakrabarti^{1,3}

¹School of Veterinary Medicine and Science, University of Nottingham, Sutton Bonington, UK

²Centre for Analytical Bioscience, Advanced Materials and Healthcare Technologies Division, School of Pharmacy, University of Nottingham, Nottingham, UK

³MRC Versus Arthritis Centre for Musculoskeletal Ageing Research, UK

Correspondence to: Lisa Chakrabarti; **email:** lisa.chakrabarti@nottingham.ac.uk

Keywords: mitochondria, Eicosanoid, cytokines, Parkinson's disease, sex differences

Received: June 4, 2020

Accepted: August 1, 2020

Published: August 27, 2020

Copyright: Ingram et al. This is an open-access article distributed under the terms of the Creative Commons Attribution License (CC BY 3.0), which permits unrestricted use, distribution, and reproduction in any medium, provided the original author and source are credited.

ABSTRACT

Response to inflammation is a key determinant in many diseases and their outcomes. Diseases that commonly affect older people are frequently associated with altered inflammatory processes. Neuroinflammation has been described in Parkinson's disease (PD) brain. PD is characterized by the loss of dopaminergic neurons in the substantia nigra pars compacta and at the sub-cellular level, mitochondrial dysfunction is a key feature. However, there is evidence that a different region of the brain, the cerebellum, is involved in the pathophysiology of PD. We report relative levels of 40 pro- and anti-inflammatory cytokines measured in PD and control cerebellar mitochondria. These data were obtained by screening cytokine antibody arrays. In parallel, we present concentrations of 29 oxylipins and 4 endocannabinoids measured in mitochondrial fractions isolated from post-mortem PD cerebellum with age and sex matched controls. Our oxylipin and endocannabinoid data were acquired via quantitation by LC-ESI-MS/MS. The separate sample sets both show there are clearly different inflammatory profiles between the sexes in control samples. Sex specific profiles were not maintained in cerebellar mitochondria isolated from PD brains.

INTRODUCTION

Though Parkinson's disease (PD) is a single diagnosis, it presents as a heterogeneous disorder with some patients experiencing a more akinetic phenotype with prevailing rigidity where others may be less affected by rigidity but have a more tremor dominant disease [1]. The measurement of these different forms is now possible using MRI and reveals that certain neural loops, for example a 'cerebello-thalamo-cortical loop' can be associated with specific symptomology [2, 3]. There is mounting evidence to justify extending the study of PD from the basal ganglia to include connecting pathways to the cerebellum [4, 5]. However, moving our attention to the cerebellum where there is

no overt cell loss warrants a careful understanding of what is happening in this region of the brain at a molecular and cellular level; this fits with recent proposals that the cerebellum is due for greater attention in the field of PD [5–7].

Mitochondrial dysfunction is a key feature of ageing and neurodegenerative disease [8, 9]. The link between mitochondrial dysfunction and disease is particularly well described in PD where it has been linked to both familial and sporadic forms. Mitochondria in PD have been shown to undergo bioenergetic changes, DNA mutations, misregulation of fission and fusion and dynamics more generally; mutations in mitochondrial proteins Parkin and PINK1 are implicated in PD [10]. A

direct link between parkin and PINK1 and the STING inflammatory pathway connects pathways central to mitochondrial dynamics and neuroinflammation [11, 12]. The alpha-synuclein protein is regarded as central to PD pathology and has been implicated in neuroimmune response while also being involved in mitochondrial dysfunction. Mitochondrial associated membranes (MAMs) and mitochondrial damage-associated molecular patterns (mtDAMPs) also directly connect mitochondria in processes leading to changes in inflammatory response [13, 14].

In PD it is accepted that more males than females have the disease, with some studies calculating a nearly 2:1 ratio between sexes [15]. It is certainly possible that oestrogen may offer neuroprotection in females but direct evidence for this in PD is not yet forthcoming [16]. However, not only are females less likely to be diagnosed with Parkinson's disease but sex differences are apparent in aspects of symptomology associated with this disease, for example swallowing disturbances, and dementia are associated more with male patients. Furthermore, normal human basal ganglia are sexually dimorphic, which might influence the onset and progression of PD [15]. When treating PD, it is apparent that there are sex differences in bioavailability of levodopa (the most potent medication for PD) even in much older post-menopausal patients. Females retain a higher availability for the drug than males with matched disease duration [17]. Sex differences in disease susceptibility and phenotype are evident in the clinic, but the molecular explanations for these are not established.

Lipid profiling by mass spectrometry allows the absolute quantitation of biologically active molecules in complex tissue preparations [18]. Oxylipins are a group of metabolites produced via oxidation of polyunsaturated fatty acids (PUFAs) [19], they have been linked to pathways of inflammation, pain and ageing [20–22]. In PD mis-folding of the protein alpha-synuclein is associated with dopaminergic cell death in the *substantia nigra*. Studies of the interaction of alpha-synuclein with PUFAs has indicated a protective role for alpha-synuclein in the inhibition of harmful oxidation reactions which affect the PUFAs [23, 24].

Arachidonic acid (AA) signalling is upregulated in the caudate-putamen and frontal cortex of unilaterally 6-hydroxydopamine (6-OHDA) lesioned rats, a model for asymmetrical PD [25]. Arachidonic acid and its derivatives are modulated in inflammation and oxidative stress and these are factors associated with induction of neurodegeneration in age-related neurological disorders [26]. Signs of inflammation are

found in many neurodegenerative diseases and can be attributed to interactions between glial and neuronal cells, activated by microglia and astrocytes [27, 28]. Pro-inflammatory cytokine contributions to the inflammasome associated with PD could be potential targets for therapy [29, 30]. However, the role of inflammation and the specific molecular signatures found in healthy ageing versus neurodegeneration must be delineated and understood throughout the brain, before therapies to regulate cytokine production can be promoted [31, 32].

Our study looked at molecular markers of inflammation measured in mitochondrial fractions derived from cerebellum to reveal whether there is a disease related process that connects with PD in this part of the human brain.

RESULTS

Variability in cytokine and oxylipin levels characterize the female control group

Highly variable inflammatory cytokine expression was measured across female control cerebellar mitochondria when compared with the equivalent male control group (Figure 1A). Of the forty cytokines interrogated on the slide arrays, twenty-one inflammatory cytokines had different variance (*f*-test) between female and male controls, only one of these (IL-1 β) had a greater variance in males. Both pro- and anti-inflammatory molecules were largely found to show greatest variance in female control groups (for comprehensive graphs see Supplementary Figure 2 and datasets Table 6). Several very highly significant differences in pro-inflammatory molecules were found including IL-12p40, MIG and TNFRI (for abbreviations of molecules measured throughout see Supplementary Table 2). Very highly significant differences in variation were also found in anti-inflammatory cytokines including IL-10 and IL-12p70. Measurements of mean levels identified pro-inflammatory cytokines RANTES ($p=0.007$) and GM-CSF ($p=0.0418$) as significantly higher in female controls when compared with age-matched male control cerebellar mitochondria (Figure 1C).

Significant differences in variance between female and male control oxylipin concentrations were found in AA, LA and pro-inflammatory 5-HETE, 9-oxoODE, 9-HODE, 8-HETE, 8,9-EET, and also anti-inflammatory 13oxoODE and 13-HODE (Figure 1B – and for comprehensive graphs see Supplementary Figure 1 and datasets Table 4). Again, the female control group showed the greater levels of variance in each case.

Fewer sex differences are found in cytokines and oxylipins of PD Braak 5-6 cerebellar mitochondrial fractions

Comparison of cerebellar mitochondria isolated from severely affected brain tissues shows fewer differences between the sexes. However, some molecules still present with different variation in levels. Cytokines measured with different variance between the sexes were pro-inflammatory MIP1 α , MIP1 β and TNF α which all showed a higher variance across the female Braak 5-6 group (Figure 1D and see Supplementary Table 6 for *f*-test data). Anti-inflammatory cytokines IL-4 and IL-12p70 showed a similar pattern of higher variance in female samples. For MCSF and TIMP-1 the male group has a greater degree of variation in cytokine levels than that found in females.

Of the oxylipins measured, just two show a difference in variation between the sexes in PD Braak 5-6 groups, both have a greater variation across the male group PD Braak 5-6 (Figure 1E). 12-HPETE an anti-inflammatory oxylipin, is found to have a higher variation across the male PD Braak 5-6 group, this is also the case for the only other oxylipin to show a difference, 5,6-EET (see Supplementary Table 4 for *f*-test data).

Endocannabinoid levels show greater variance in the control female group

Though there are multiple reviews and studies on the effect of endo/cannabinoids on brains of mammalian models of PD [33, 34], the measurement of endocannabinoid species in human post-mortem PD brain has not been reported. Reflecting the datasets gathered from the oxylipin and cytokine measurements, we found that there was no mean difference between the four groups in the endocannabinoid species that were analysed (Figure 1F and Supplementary Table 7). However, once again the *f*-test showed there was a significant difference in variation when comparing the female group data with the PD Braak 5-6 female group in 3 of the four endocannabinoid species, namely 2-AG, AEA and PEA.

The female PD group is characterized by a reduction in inflammatory markers

Comparison of cerebellar mitochondrial oxylipin levels in female PD Braak 5-6 fractions with controls shows a significant reduction in the levels of thirteen oxylipins (Figure 2A). AA and pro-inflammatory molecules 12-HETE, TXB2, 5-HETE, 5-HPETE, 12-HPETE, 9-HODE and 9-oxoHODE are all significantly reduced in the PD females. Also, five oxylipins with anti-inflammatory roles were significantly reduced in the PD female samples these were 5,6-EET, 16-HETE, 17-

HDoHE, 13-HODE and 13-oxoODE (see Supplementary Table 3 for *p* values).

Two cytokines, one pro-inflammatory ICAM-1 ($p=0.0274$) and the other anti-inflammatory TIMP-2 ($p=0.036$) were found to be significantly reduced in PD females when compared with controls (Figure 2B and Supplementary Table 5).

Variation in levels of oxylipins in the female control group is attenuated in PD cerebellar mitochondria

Comparison of oxylipin levels in control and PD Braak 5-6 groups showed that the variation of oxylipin levels that characterize the female control cerebellar mitochondria is much reduced in the PD Braak 5-6 group. Eleven oxylipins showed a significant reduction in variation (*f*-test) in the PD group, these were LA and PGE2; pro-inflammatory molecules 5-HETE, 5-HPETE, 12-HPETE, 9-oxoODE, 9-HODE, 5,6-EET and 17-HDoHE; anti-inflammatory oxylipins 13-oxoODE and 13-HODE (Figure 2C also Supplementary Figure 1 and Table 4).

Free fatty acids and PTGS2 levels are significantly altered in male PD Braak 5-6 cerebellar mitochondrial fractions

We measured total free fatty acid levels in the cerebellar mitochondria from control, PD Braak 3-4 (more moderate pathology) and PD Braak 5-6 brains. Though the numbers of samples were limited there was an upward trend in the PD Braak 3-4 samples, becoming a significant increase in free fatty acid content ($p=0.0164$) in the more severely affected PD Braak 5-6 derived samples (Figure 3A). The enzyme prostaglandin synthase 2 (PTGS2, also known as cyclooxygenase 2 or COX2) has a role in regulating inflammatory processes and is found to be increased in dopaminergic neurons of the *substantia nigra* in PD [35]. PTGS2 had not been previously measured in the cerebellar mitochondria of PD brains. In cerebellum samples we saw no change in PTGS2 levels in PD Braak 3-4 samples, however a significant drop in the levels of this enzyme in PD Braak 5-6 samples ($p=0.0307$) was measured (Figure 3B).

A pattern of higher levels of oxylipins is seen in PD Braak 3-4 males

Many of the oxylipin species measured had a pattern of increased levels in Braak 3-4 male cerebellar mitochondria when compared with controls and Braak 5-6 samples (figure 3C). A selection of the species that exhibited this pattern are shown, including LTB4 where significance is reached between samples from PD Braak 3-4 and PD Braak 5-6 ($p=0.0139$).

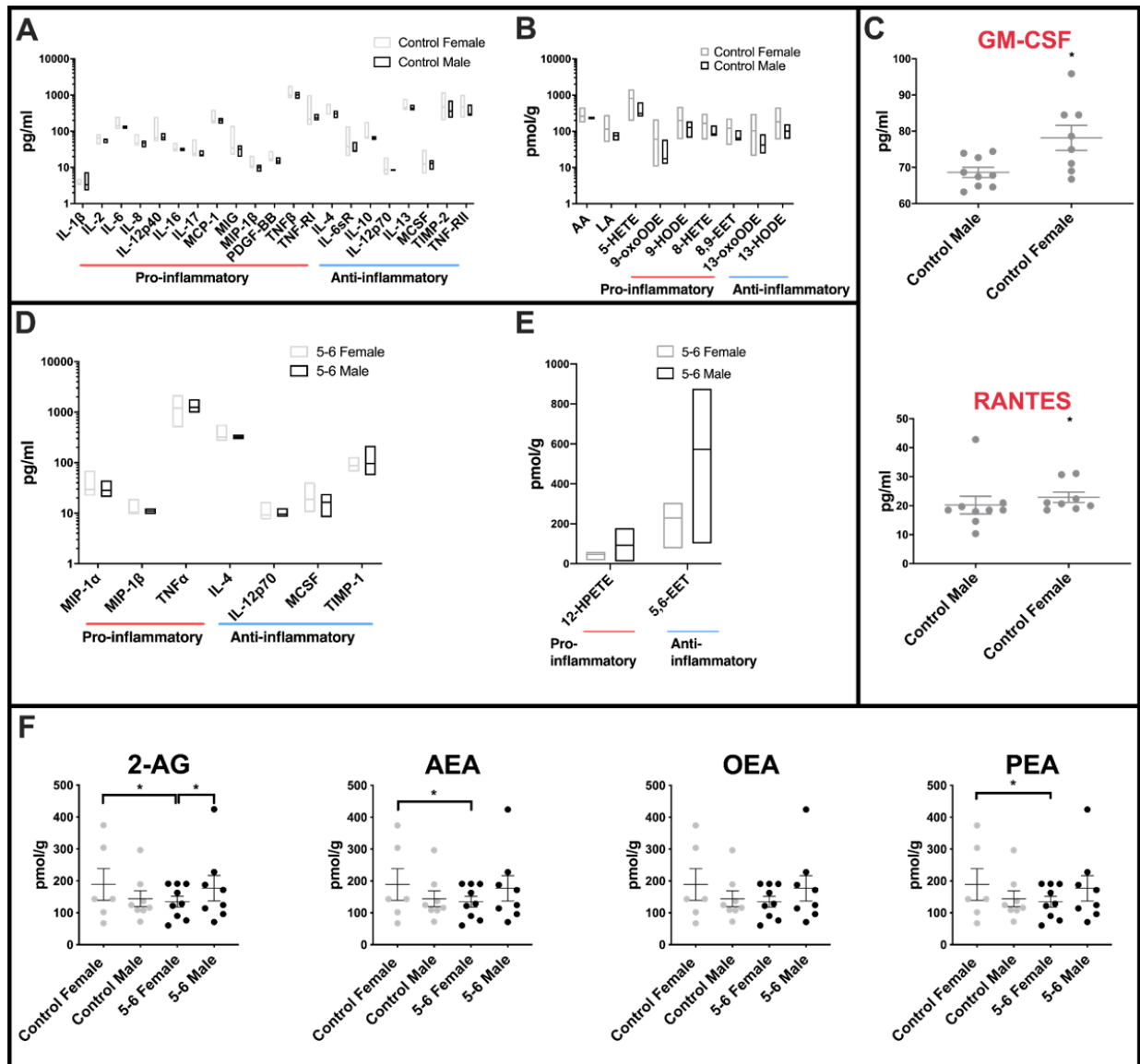


Figure 1. Sex differences in inflammatory profiles of cerebellar mitochondria. (A) Cerebellar mitochondria of female controls have highly variable inflammatory cytokine expression compared with male controls. Twenty-one inflammatory cytokines showed significantly different variance between female and male controls. Twenty of these were significantly more variant in females. Control male n=9; control female n=8. (B) Oxylipin variance is significantly greater in cerebellar mitochondria of female controls than male controls. Female controls have significantly greater variance in nine oxylipins. Male control cerebellar mitochondrial oxylipin levels are less variant within the group. Control male n=5; control female n=5. (C) Two inflammatory cytokines are significantly increased in female compared to male controls. RANTES and GM-CSF were significantly increased in mean levels in female controls compared to male controls. Control male n=9; control female n=8. (D) Cerebellar mitochondria from PD Braak 5-6 females have greater variability in inflammatory cytokine expression than the Braak 5-6 males. Six of seven significant inflammatory cytokines showed higher variance in the PD Braak 5-6 female group than PD Braak 5-6 males. PD Braak 5-6 male n=10; PD Braak 5-6 female n=9. (E) PD Braak 5-6 males and females show little variance in all but two cerebellar mitochondrial oxylipin levels. Two oxylipins have significantly higher variance values in PD Braak 5-6 males than females. PD Braak 5-6 male n=5; PD Braak 5-6 female n=5. All samples were age matched. A, B, D and E present inflammatory cytokine and oxylipins with significantly different variances (*f*-test). Refer to Supplementary Tables 4 and 6 for *f* values of oxylipins and inflammatory cytokines, respectively. Box plots display interleaved high and low. The horizontal line represents the mean. C shows significantly altered cytokines. Red title font represents pro-inflammatory cytokine. Displayed are mean levels \pm SEM. (Mann-Whitney U-test). Refer to Supplementary Table 5 for *p* values. (F) Endocannabinoid variance is reduced in PD Braak 5-6 females. Female control group has heterogenous quantities of 2-AG, AEA and PEA compared with PD Braak 5-6 female group. Males do not show significant variation in endocannabinoid levels. Statistical analyses were carried out using GraphPad Prism (*f*-test). No significant differences were seen between the means of the groups (Kruskal-Wallis test with multiple comparison's). Braak 5-6 male n=8; Braak 5-6 female n=9; control male n=8; control female n=6. All samples were age matched. Plots display mean \pm SEM. Bars above plots represent statistically significant differences. Refer to Supplementary Table 7 for *p* and *f* values.

Arachidonic acid levels vary in PD cerebellar mitochondria

AA is metabolized through well characterized pathways to generate a range of oxylipin species [18]. In control males we see quite similar and consistent levels of AA across the samples that were analysed (Figure 3C). However, there is significantly more variation in AA levels in both the PD Braak 3-4 samples ($p=0.0072$) and the PD Braak 5-6 samples ($p=0.0209$) when compared with controls (for f -test values see Supplementary Table 4).

Mean levels and variation of levels of cytokines are increased in male PD Braak 5-6 cerebellar mitochondria

Pro-inflammatory cytokines Eotaxin-1, I-309, IL-1 β , IL-12p40, MIG, TNF RII, and anti-inflammatory IL-1ra and IL-12p70 were each found at significantly higher mean levels in the male PD Braak cerebellar mitochondria samples than in matched controls (Figure 4A: for p values see Supplementary Table 5). The variation across the PD Braak 5-6 group was also much greater than across the control group (Figure 4B and for f -test values see Supplementary Table 6). Pro-inflammatory cytokines BLC, Eotaxin, GM-CSF, I-309, IL-2, IL-6, IL-7, IL-12p40, IL-15, MIP-1d, PDGFB, RANTES, TNF RI, and anti-inflammatory cytokines IL-5, IL-10, IL-12p70, MCSF and TNF RII each had significantly greater variance in levels across the PD Braak 5-6 group compared with controls.

DISCUSSION

Though much has been determined about PD associated changes in the cerebellum using imaging techniques, specific molecular and pathological evidence is scant [1, 36, 37]. Epigenetic changes in PD cerebellum have been investigated and give good reason to anticipate that regulatory pathways are changed during the disease course [6, 38]. Mitochondrial dysfunction is a key feature of PD. Our molecular analyses of mitochondrial fractions now show quite clearly that there are disease associated changes of inflammation pathways in PD cerebellum.

Inflammatory processes in the context of PD have suddenly been placed in the spotlight with the discovery that mitophagy proteins PINK1 and Parkin (both are implicated in familial PD) are important for regulating innate immunity and inflammation as shown in rodent models [11, 39]. We are the first to quantify molecular changes consistent with dysregulation of inflammatory processes in mitochondrial fractions of post-mortem human cerebellum. The role of neuroinflammation in

PD is going to take some unravelling, but our data establish the cerebellum as a region that is affected in the disease process. Neuroinflammation has been shown to commence early in PD, peaking in moderately affected individuals, this fits with our data on PD Braak 3-4 subjects [40]. CSF and plasma DHA derived resolvin D1 (RvD1) are reduced in patients with early-onset PD [41], suggesting that inflammation resolution processes could be dysfunctional. We find the picture is complex, as should be expected, with both anti- and pro-inflammatory processes activated simultaneously to tune a potentially compensatory response to disease.

Sex differences in PD are recognized but have not been investigated thoroughly, particularly from a biochemical aspect [42–44]. Differences in development of the immune system and lifelong neuro-epigenetic differences in brain inflammatory profiles have been explored in rodents but the extent to which these findings translate to the human brain is not clear [45]. Specifically interesting in PD is the role of the testis-determining factor gene SRY [46]. In mouse, the SRY gene promotes catecholamine production by dopaminergic neurons of the substantia nigra [47], and rat models with repressed SRY expression show protection from experimentally induced PD [48]. A recent analysis shows an elevated prevalence of PD in females with the LRRK2 G2019S mutation [49]. Sexual dimorphism has been observed in the inflammatory response to traumatic brain injury in rodents [50, 51], and there is some limited information on sex differences in eicosanoid biology [52]. It is suggested that females can mount a more acute and efficient immune response, and subsequently resolve it more effectively than males [53–55]. The heterogeneity we see in the levels of inflammatory molecules in female controls could be responsible for the delay in onset and other phenotypic sex differences in PD. We found RANTES, a chemokine that induces infiltration into T-cells, to be significantly increased in female control cerebellar mitochondria compared with males. Decreasing RANTES in the *substantia nigra* has been shown to prevent loss of dopaminergic neurons in mouse models of PD [56]. In human PD, post-mortem *substantia nigra* contains more RANTES confirming association with disease but not necessarily with cell death in this region. From our study it is difficult to tell whether control females with low levels of the markers that are significantly more varied in the female control group, are at a higher risk for PD in the future. We show that sex differences are important to define in all studies of PD. Sex specific datasets can give clues about disease mechanism and pave the way to personalized medical approaches. Measurement of many markers of inflammatory processes in our study show that the control female groups have a greater range of these

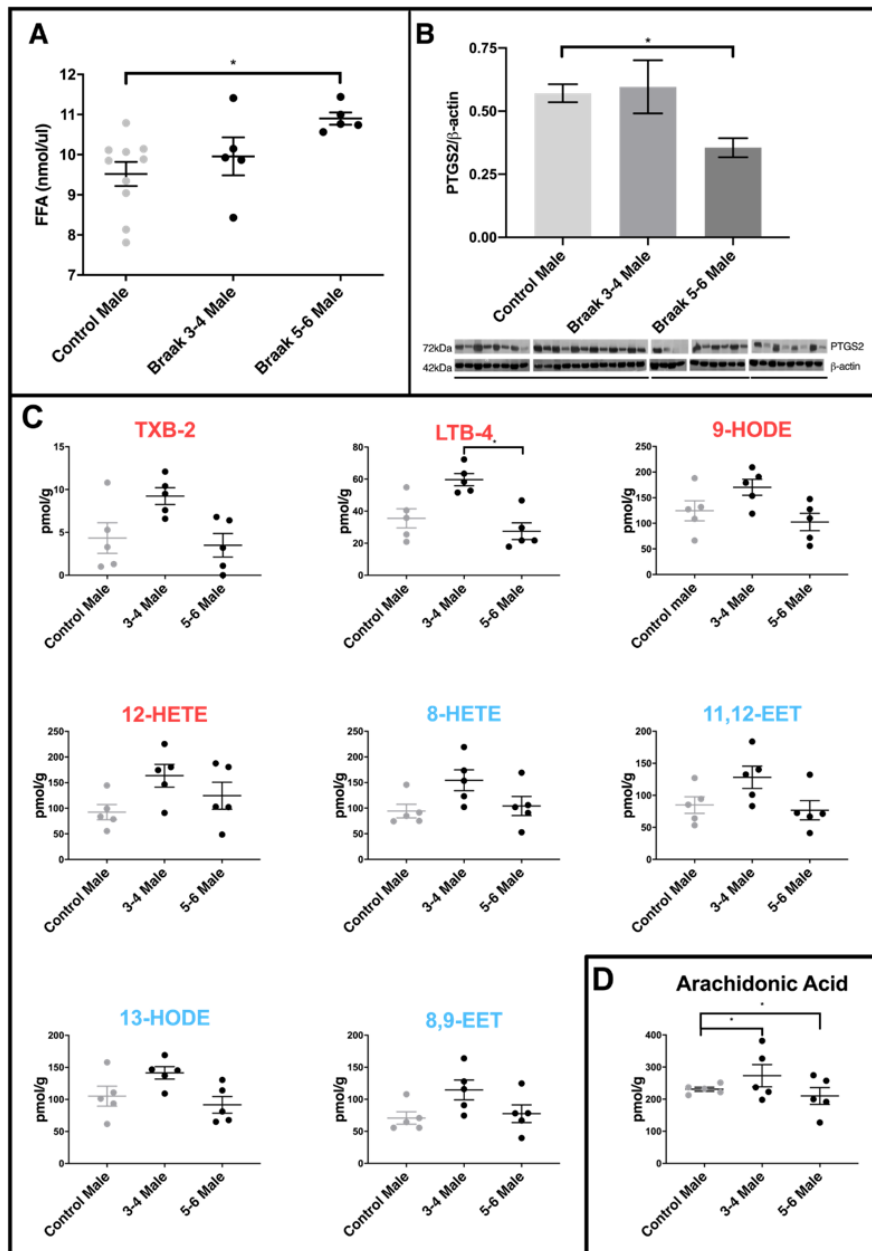


Figure 3. Comparison of PD cerebellar mitochondria with different Braak classification. (A) Free fatty acid concentration is increased in cerebellar mitochondria of PD Braak stage 5-6 males. A significant increase in FFA levels was shown in cerebellar mitochondria of Braak stage 5-6 males compared to age-matched controls ($p=0.0164$). No significant differences were apparent between PD Braak stage 3-4 and control. PD Braak 3-4 males ($n=5$), PD Braak 5-6 males ($n=5$), age-matched control males ($n=10$). Plots show mean values (nmol/μl) ± SEM (Kruskal-Wallis test with multiple comparisons). (B) Cerebellar levels of PTGS2 in PD Braak 5-6 mitochondrial fractions are lower compared with PD Braak 3-4 and controls. PTGS2 measured in enriched mitochondrial fractions were present in significantly lower quantities in the cerebellum of PD Braak 5-6 males compared to male controls ($p=0.0307$). No significant difference in PTGS2 levels were seen between PD Braak 3-4 and age-matched control. Mitochondrial PTGS2 levels, normalized to β-actin, were determined by Western blotting using mitochondrial and cytosolic fractions extracted from cerebellar tissue from age-matched male control ($n=10$) and PD Braak 3-4 ($n=5$) and 5-6 ($n=4$). Columns show the mean ± SEM (Kruskal-Wallis test with multiple comparisons). (C) Oxylipin concentrations in cerebellar mitochondria. LTB-4 is significantly decreased in PD Braak 5-6 males ($n=5$) compared to PD Braak 3-4 males ($n=5$); $p=0.0139$ (Kruskal-Wallis test with multiple comparisons). No significant differences were apparent between PD male groups and age-matched male controls ($n=5$). Red /blue titles represent pro- /anti-inflammatory, respectively. No significant changes were found between control males and PD Braak 5-6 males. Plots display mean concentration (pmol/g) ± SEM. Refer to Supplementary Table 5 for all p values (Kruskal-Wallis test with multiple comparisons). (D) Arachidonic acid levels in PD. Cerebellar mitochondrial arachidonic acid levels are similar in control males but significant variation is seen in PD Braak 3-4 and 5-6 males. Refer to Supplementary Table 4 for f values. All samples were age matched. PD Braak 3-4 male $n=5$; PD Braak 5-6 male $n=5$; control male $n=5$.

molecules with significantly higher mean levels. The greater range seen in females is interesting and needs to be explored further. It may be that younger females have generally high levels and the lower values seen in these age groups reflect a reduction associated with increased age. All this leads to the suggestion that neuroinflammatory responses measured as increases in oxylipins and cytokines, may be a protective state or acute response which changes or becomes exhausted in

chronic disease states [57, 58]. This is potentially supported by the data shown for trends in the male groups where we were able to measure levels of oxylipins in control, PD Braak3-4 and PD Braak 5-6 cerebellar mitochondria. Though significance was only reached in the case of LTB-4 there was a trend towards an increase in levels of inflammatory molecules at the earlier disease stage (PD Braak 3-4), which was abated in the more severely affected PD Braak 5-6 group. The

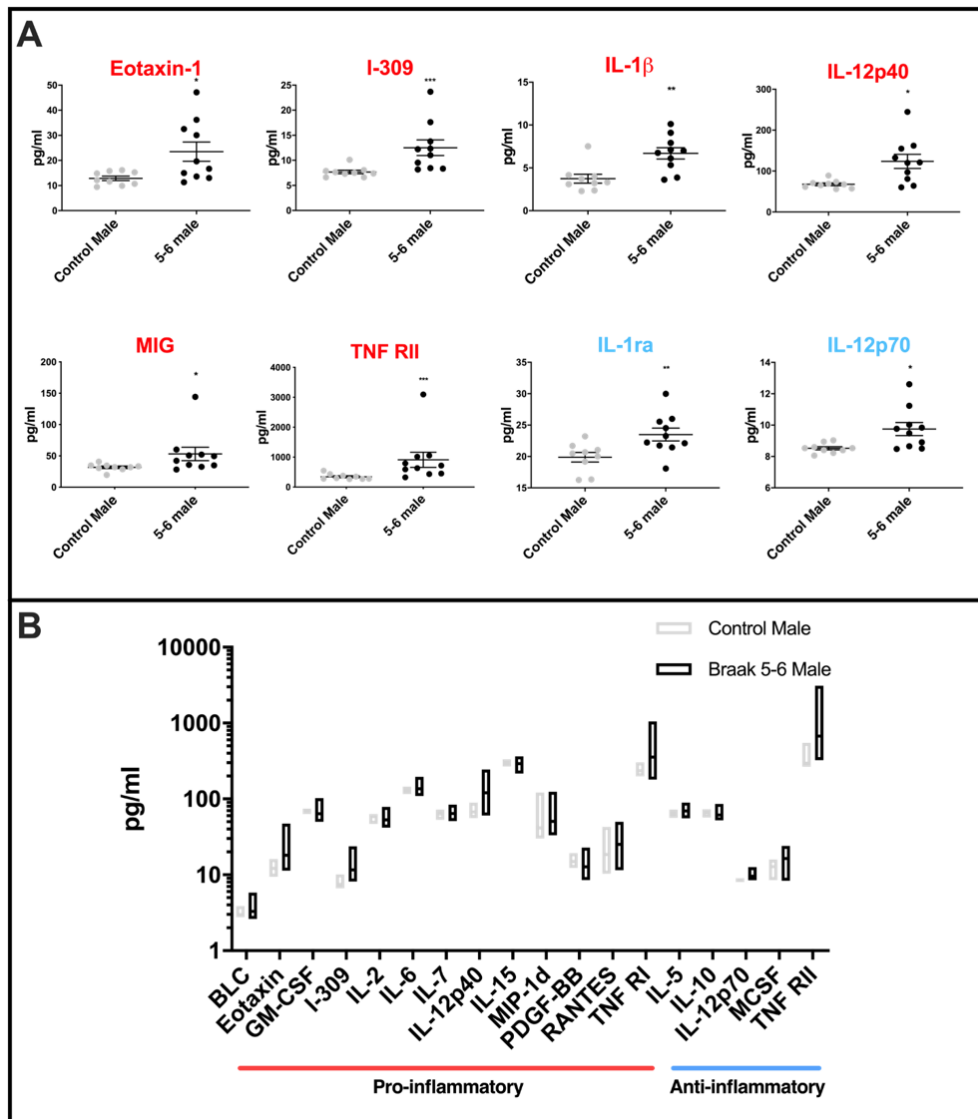


Figure 4. Cytokine levels in PD Braak 5-6 male cerebellar mitochondria (A) Mean levels of cytokines are higher in cerebellar mitochondria of PD Braak 5-6 males. Eight inflammatory cytokines were increased in cerebellar mitochondria of PD Braak 5-6 males compared with control males. PD Braak 5-6 male n=10; control male n=9. Red or blue titles represent pro- /anti-inflammatory, respectively. Plots display mean concentration (pg/ml) ± SEM (Mann-Whitney test), see Supplementary Table 5 for *p* values (Mann-Whitney U test). (B) PD Braak 5-6 males show different variance in cerebellar mitochondrial cytokines levels than was seen in the control male group. All seventeen measured inflammatory cytokines with significant differences in variance are more dispersed from the mean in PD Braak 5-6 males than control males. PD Braak 5-6 male n=10; PD Braak 5-6 female n=9; control male n=9; control female n=8. Box plots display interleaved high and low. The horizontal line represents the mean. Data shown are oxylipins (A+B) with significant variances (*f*-test). Refer to Supplementary Table 6 for *f* values.

reduced range, or flat level of the molecules being measured in PD Braak 5-6 males is striking. This is a stage of disease that is clearly advanced with massive cell losses in the substantia nigra, it may be that the inflammatory response has been exhausted in the earlier stages of the disease. LTB-4 has been implicated previously in PD studies [59], but due to the poor correlation of rodent model PD to human disease it is difficult to draw any real conclusions about its precise role in the process.

Patterns of cytokine levels add further to the complexity of the picture of neuroinflammation in PD. Mean increases of both pro- and anti-inflammatory cytokines in cerebellar mitochondria could be used to define the male PD Braak 5-6 group. The most significant of these increases were in the pro-inflammatory molecules I-309 and TNF RII, followed by IL-1 β and anti-inflammatory IL-1ra. TNF-RII antagonists have been proposed to have a therapeutic effect upon PD disease pathways, suggesting that this increase may be initiated in the cerebellum to compensate disease process in the *substantia nigra* [60]. Similar proposals have been made with respect to the cytokine I-309 [61]. There are a few studies on IL-1 β and IL-1ra in the context of PD, supporting the idea of inflammatory responses in brain regions other than the *substantia nigra*.

We have compiled a molecular profile of inflammation in PD cerebellar mitochondria. This study emphasizes that there are interesting molecular changes in the cerebellum that correlate with PD. Our findings highlight the need to establish sex specific differences in disease at the molecular level when these are recognized in the clinical phenotype.

MATERIALS AND METHODS

Human post-mortem cerebellar samples

This study was performed with ethical approval from Parkinson's UK Brain Bank and University of Nottingham SVMS Ethics committee (Reference# 2035 170519). Please see Supplementary Table 1 for information on patients and controls used in this study. Cerebellar mitochondria were isolated from 24 control, and 34 PD post-mortem brains. PD cases were further classified into Braak stages 3-4 and 5-6 respectively. Braak staging was assigned at the Parkinson's UK Brain Bank according to published classification [62]. Oxylipin and cytokine profiling experiments used different post-mortem brain sample sets precluding sample group specific conclusions.

Mitochondrial isolation

Enriched mitochondrial fractions were separated by differential centrifugation according to our previously

published protocols [63]. Briefly, previously flash frozen cerebellar samples were placed in GentleMACS C tubes with mitochondria extraction buffer (50 mM Tris-HCl pH7.4, 100 mM KCl, 1.5 mM MgCl₂, 1 mM EGTA, 50 mM HEPES and 100 mM sucrose; all sourced from Sigma-Aldrich, UK) and homogenized using a GentleMACS Dissociator (Miltenyi Biotec). The resulting homogenates were spun at 4°C in an Eppendorf Model 5417R Microcentrifuge (Fisher Scientific); first at 850 x g for 10 minutes, then the supernatant obtained was centrifuged separately at 1000 x g for 10 minutes to yield a nuclear pellet and a final spin at 10000 x g for 30 minutes to produce the mitochondrial pellet; the remaining supernatant contained the cytosolic fraction. Fractions were stored at -80°C.

Protein assay

The protein concentrations of the samples were determined using the Bradford Assay - Sigma [64]. Bovine serum albumin (BSA- Fisher Scientific) standards of known protein concentration varying from 0 to 2mg/ml were added to Bradford reagent in disposable cuvettes (Fisher Scientific) and the absorbance was measured spectrophotometrically at 595 nm in a Thermo Scientific Spectrometer Helios Epsilon (Fisher Scientific). The absorbance of the known protein standards was plotted using linear regression. The mitochondrial fractions were diluted 1 μ l in 100 μ l Tris Buffer and added to Bradford reagent before the absorbance was measured. The absorbance was plotted against the BSA standard curve to determine the estimated protein concentration (mg/ml).

Western blot

Western blotting for quality control of fractions was carried out as described previously [65]. Antibody dilutions: PTGS2 ab62331 (Abcam) 1:2000 dilution in 5% (w/v) BSA in 1xTBS-T; β -actin ab8227 (Abcam) in 5% (w/v) BSA in 1xTBS-T; Goat anti-Rabbit IgG (HRP) A16096 (Invitrogen) 1:1000 in 5% (w/v) BSA in 1xTBS-T. Mitochondrial fractions were normalized to β -actin level. Blots were visualized using ChemiDoc MP Imaging System (Bio-Rad) and ECL Plus reagent (Pierce). Densitometry was carried out using ImageJ. Statistical analyses were carried out in GraphPad Prism.

Free fatty acid quantitation

Total fatty acid concentration was measured using a Free Fatty Acid Quantification Kit (AB65341, Abcam), according to manufacturer's instructions. Fatty acid concentrations were quantified by fluorometric analysis (Varioskan LUX Multimode Microplate Reader).

Oxylipin quantitation

LC-ESI-MS/MS was used for analysis of oxylipins (AA, LA, 12-HETE, TXB-2, PGE2, 5-HETE, 5-HPETE, 12-HPETE, 9-HETE, 20-HETE, LTB-4, 9-oxoODE, 9-HODE, 5,6-EET, 5,6-DHET, 8,9-DHET, 11,12-DHET, 14,15-DHET, 8-HETE, 11-HETE, 15-HETE, 16-HETE, 8,9-EET, 11,12-EET, 14,15-EET, 17-HDoHE, 13-oxoODE, 13-HODE, 8,15-DiHETE) in mitochondrial fractions of human cerebellar tissue. A gradient LC method based on that described by Wong *et al* (14) using a modular Shimadzu Vp series HPLC was used to introduce the samples. Injection volume was 20 μ l. The MS system used was a triple quadrupole ion-trap 4000 QTRAP (Sciex, UK), equipped with Turbo Spray ionization interface. Standards were purchased from Cambridge Biosciences, Cambridge, UK. One batch of QC human plasma standard samples (from in-house stock) was used to confirm the intra-day accuracy of the method.

Endocannabinoids quantitation

LC-ESI-MS/MS was used for analysis of endocannabinoids: arachidonyl ethanolamide (anandamide, AEA), 2-arachidonyl glycerol (2-AG), palmitoyl ethanolamide (PEA), oleoyl ethanolamide (OEA) in mitochondrial fractions of human cerebellar tissue. A uHPLC system, a modular Exion series LC (Sciex, Warrington, UK) was used to create a 10 min gradient and introduce the 5 μ l sample. The column (uPLC BEH C18 1.7 μ m (2.1x150mm, Waters, Elstree, UK) was held at 60°C [66]. The MS system used was a Qtrap 6500+ (Sciex, Warrington, UK) equipped with an electrospray ionization (ESI) interface. Standards were purchased from Cambridge Biosciences, Cambridge, UK. One batch of QC human plasma standard samples (from in-house stock) was used to confirm the intra-day accuracy of the method.

Human inflammation antibody array

Abcam human inflammation antibody array (ab197451) kit was used for the detection of 40 cytokines: BLC, eotaxin-1, eotaxin-2, G-CSF, GM-CSF, I-309, ICAM-1, IFN γ , IL-1 α , IL-1 β , IL-1ra, IL-2, IL-4, IL-5, IL-6, IL-6sR, IL-7, IL-8, IL-10, IL-11, IL-12p40, IL-12p70, IL-13, IL-15, IL-16, IL-17. MCP-1, MCSF, MIG, MIP-1 α , MIP-1 β , MIP-1 δ , PDGF-BB, RANTES, TIMP-1, TIMP-2, TNF α , TNF β , sTNF RI, sTNF RII (guide to abbreviations in Supplementary Table 2). Glass slides contained 16 identical antibody arrays, with a 16 well gasket for addition of separate samples to each array. Antibodies were spotted in quadruplicate in each array. Protocol was followed as per manufacturer's instructions. Briefly, gasket wells were blocked for 30

minutes in Sample Diluent, followed by addition of a standard cytokine cocktail or 100ug of sample, diluted in PBS. The cocktail of standard cytokines was diluted three-fold across eight dilutions and 100ul was added to each well for 60 minutes. Slides were washed in supplied wash buffer 7 times for 5 minutes each, with gentle agitation at room temperature. The detection antibody was reconstituted in 1.4ml sample diluent and 80ul added to each well and incubated overnight at 4°C, with gentle agitation. Subsequently, another 7 washes were carried out, as described above. 80ul of Cy3 equivalent dye-conjugated streptavidin was added to each well. At this step, the slide was covered in aluminium foil to avoid exposure to light and incubated at room temperature for 1 hour. A further 5 wash steps for 5 minutes each followed. A final 2 wash steps were carried out for 15 minutes each. Finally, slides were completely dried with 3 times 3-minute centrifugation steps at 1,000rpm. For signal visualization, slides were scanned at 532nm and data analysed using GenePix Pro Software (Axon GenePix). The median local background was subtracted from the median fluorescence of each spot and the corrected fluorescence was used to calculate the average fluorescence signal as well as the standard deviation.

Statistical analysis

Data from the various experiments were presented as mean average alongside calculated standard deviation and standard error mean. Mann-Whitney U and Kruskal-Wallis tests were performed on the datasets using GraphPad Prism version 6 for Windows (GraphPad Software, San Diego California USA).

ACKNOWLEDGMENTS

This research could not have been performed without the generosity and trust of the individuals who donated their brains and their families who agreed to comply with their wish to support the Parkinson's UK Brain Bank. We are grateful to the brain bank for arranging access to these precious samples and particularly to Djordje Gveric for smooth communication and facilitation of sample access.

AUTHOR CONTRIBUTIONS

TLI (stxtli@nottingham.ac.uk) performed experimental work and prepared the manuscript, FS (mdzfds@nottingham.ac.uk) prepared and received samples and performed experimental work, SS (pazss2@nottingham.ac.uk) performed endocannabinoid profiling, CO (pazco@nottingham.ac.uk) performed and supervised mass spectrometry experiments and helped interpret data and prepare the manuscript, DB

(paadb1@nottingham.ac.uk) provided expertise, directed mass spectrometry experiments and helped with data interpretation and manuscript preparation, LC directed the research, supervised experiments, provided reagents and prepared the manuscript.

CONFLICTS OF INTEREST

The authors declare they have no conflicts of interest.

FUNDING

This work was supported by the Biotechnology and Biological Sciences Research Council [grant number BB/J014508/1], via an award to TLI.

REFERENCES

1. Zhang J, Wei L, Hu X, Xie B, Zhang Y, Wu GR, Wang J. Akinetic-rigid and tremor-dominant Parkinson's disease patients show different patterns of intrinsic brain activity. *Parkinsonism Relat Disord*. 2015; 21:23–30.
<https://doi.org/10.1016/j.parkreldis.2014.10.017>
PMID:[25465747](https://pubmed.ncbi.nlm.nih.gov/25465747/)
2. Palmer SJ, Li J, Wang ZJ, McKeown MJ. Joint amplitude and connectivity compensatory mechanisms in Parkinson's disease. *Neuroscience*. 2010; 166:1110–18.
<https://doi.org/10.1016/j.neuroscience.2010.01.012>
PMID:[20074617](https://pubmed.ncbi.nlm.nih.gov/20074617/)
3. Dirks MF, Zach H, van Nuland A, Bloem BR, Toni I, Helmich RC. Cerebral differences between dopamine-resistant and dopamine-responsive Parkinson's tremor. *Brain*. 2019; 142:3144–3157.
<https://doi.org/10.1093/brain/awz261>
PMID:[31509182](https://pubmed.ncbi.nlm.nih.gov/31509182/)
4. Seidel K, Bouzrou M, Heidemann N, Krüger R, Schöls L, den Dunnen WF, Korf HW, Rüb U. Involvement of the cerebellum in Parkinson disease and dementia with lewy bodies. *Ann Neurol*. 2017; 81:898–903.
<https://doi.org/10.1002/ana.24937>
PMID:[28439961](https://pubmed.ncbi.nlm.nih.gov/28439961/)
5. Wu T, Hallett M. The cerebellum in Parkinson's disease. *Brain*. 2013; 136:696–709.
<https://doi.org/10.1093/brain/aws360>
PMID:[23404337](https://pubmed.ncbi.nlm.nih.gov/23404337/)
6. Stöger R, Scaife PJ, Shephard F, Chakrabarti L. Elevated 5hmC levels characterize DNA of the cerebellum in Parkinson's disease. *NPJ Parkinsons Dis*. 2017; 3:6.
<https://doi.org/10.1038/s41531-017-0007-3>
PMID:[28649606](https://pubmed.ncbi.nlm.nih.gov/28649606/)
7. Yoo HS, Choi YH, Chung SJ, Lee YH, Ye BS, Sohn YH, Lee JM, Lee PH. Cerebellar connectivity in Parkinson's disease with levodopa-induced dyskinesia. *Ann Clin Transl Neurol*. 2019; 6:2251–60.
<https://doi.org/10.1002/acn3.50918> PMID:[31643140](https://pubmed.ncbi.nlm.nih.gov/31643140/)
8. Kauppila TE, Kauppila JH, Larsson NG. Mammalian mitochondria and aging: an update. *Cell Metab*. 2017; 25:57–71.
<https://doi.org/10.1016/j.cmet.2016.09.017>
PMID:[28094012](https://pubmed.ncbi.nlm.nih.gov/28094012/)
9. Area-Gomez E, Guardia-Laguarta C, Schon EA, Przedborski S. Mitochondria, OxPhos, and neurodegeneration: cells are not just running out of gas. *J Clin Invest*. 2019; 129:34–45.
<https://doi.org/10.1172/JCI120848> PMID:[30601141](https://pubmed.ncbi.nlm.nih.gov/30601141/)
10. Bose A, Beal MF. Mitochondrial dysfunction in Parkinson's disease. *J Neurochem*. 2016 (Suppl 1); 139:216–231.
<https://doi.org/10.1111/jnc.13731>
PMID:[27546335](https://pubmed.ncbi.nlm.nih.gov/27546335/)
11. Sliter DA, Martinez J, Hao L, Chen X, Sun N, Fischer TD, Burman JL, Li Y, Zhang Z, Narendra DP, Cai H, Borsche M, Klein C, Youle RJ. Parkin and PINK1 mitigate STING-induced inflammation. *Nature*. 2018; 561:258–62.
<https://doi.org/10.1038/s41586-018-0448-9>
PMID:[30135585](https://pubmed.ncbi.nlm.nih.gov/30135585/)
12. McWilliams TG, Prescott AR, Montava-Garriga L, Ball G, Singh F, Barini E, Muqit MM, Brooks SP, Ganley IG. Basal mitophagy occurs independently of PINK1 in mouse tissues of high metabolic demand. *Cell Metab*. 2018; 27:439–49.e5.
<https://doi.org/10.1016/j.cmet.2017.12.008>
PMID:[29337137](https://pubmed.ncbi.nlm.nih.gov/29337137/)
13. Hazeldine J, Dinsdale RJ, Harrison P, Lord JM. Traumatic injury and exposure to mitochondrial-derived damage associated molecular patterns suppresses neutrophil extracellular trap formation. *Front Immunol*. 2019; 10:685.
<https://doi.org/10.3389/fimmu.2019.00685>
PMID:[31001279](https://pubmed.ncbi.nlm.nih.gov/31001279/)
14. Rieusset J. Mitochondria-associated membranes (MAMs): an emerging platform connecting energy and immune sensing to metabolic flexibility. *Biochem Biophys Res Commun*. 2018; 500:35–44.
<https://doi.org/10.1016/j.bbrc.2017.06.097>
PMID:[28647358](https://pubmed.ncbi.nlm.nih.gov/28647358/)
15. Smith KM, Dahodwala N. Sex differences in Parkinson's disease and other movement disorders. *Exp Neurol*. 2014; 259:44–56.
<https://doi.org/10.1016/j.expneurol.2014.03.010>
PMID:[24681088](https://pubmed.ncbi.nlm.nih.gov/24681088/)
16. Siani F, Greco R, Levandis G, Ghezzi C, Daviddi F, Demartini C, Vegeto E, Fuzzati-Armentero MT, Blandini F. Influence of estrogen modulation on glia activation

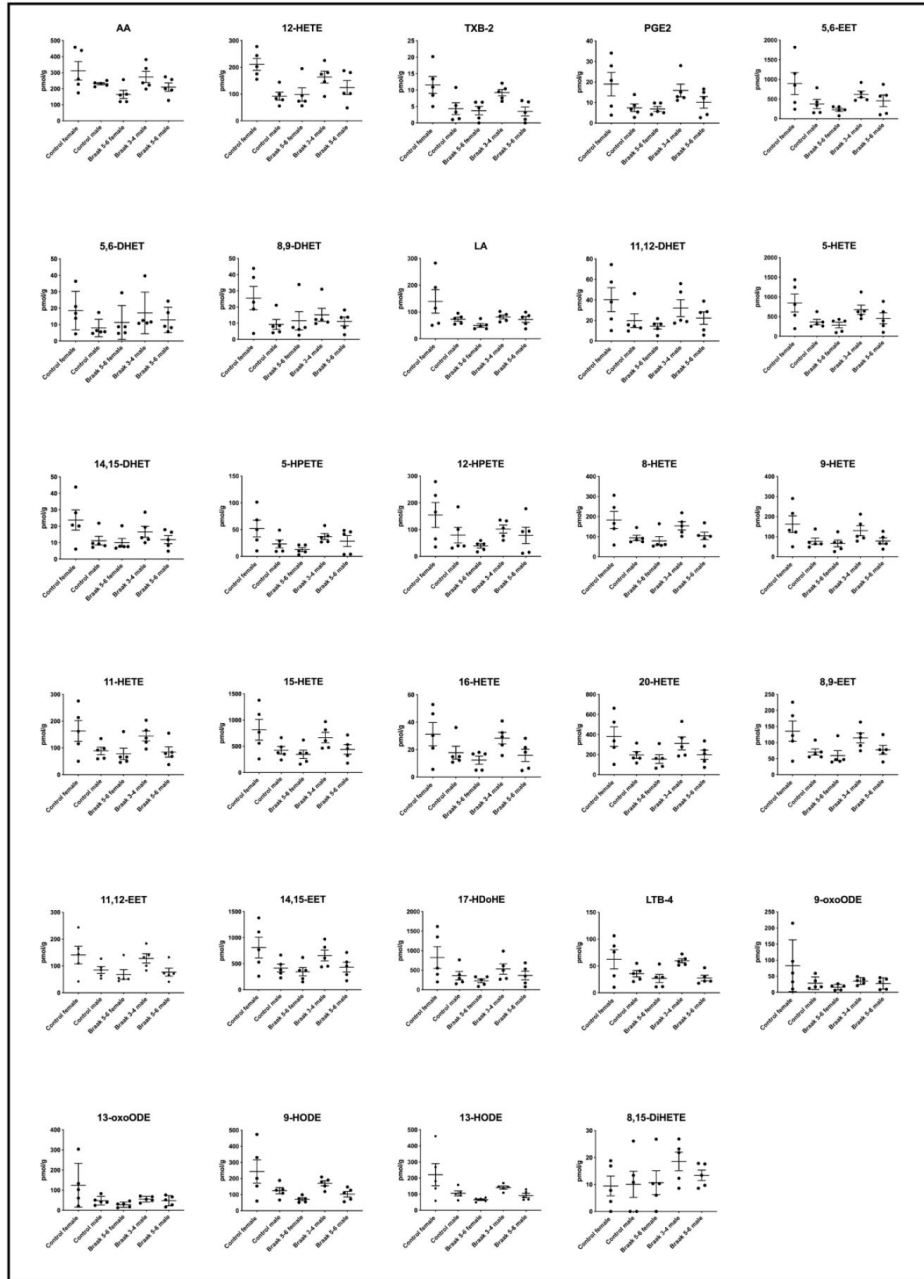
- in a murine model of Parkinson's disease. *Front Neurosci.* 2017; 11:306.
<https://doi.org/10.3389/fnins.2017.00306>
PMID:[28620274](https://pubmed.ncbi.nlm.nih.gov/28620274/)
17. Kumagai T, Nagayama H, Ota T, Nishiyama Y, Mishina M, Ueda M. Sex differences in the pharmacokinetics of levodopa in elderly patients with Parkinson disease. *Clin Neuropharmacol.* 2014; 37:173–76.
<https://doi.org/10.1097/WNF.000000000000051>
PMID:[25384078](https://pubmed.ncbi.nlm.nih.gov/25384078/)
 18. Wong A, Sagar DR, Ortori CA, Kendall DA, Chapman V, Barrett DA. Simultaneous tissue profiling of eicosanoid and endocannabinoid lipid families in a rat model of osteoarthritis. *J Lipid Res.* 2014; 55:1902–13.
<https://doi.org/10.1194/jlr.M048694>
PMID:[25062663](https://pubmed.ncbi.nlm.nih.gov/25062663/)
 19. Liakh I, Pakiet A, Sledzinski T, Mika A. Modern methods of sample preparation for the analysis of oxylipins in biological samples. *Molecules.* 2019; 24:1639.
<https://doi.org/10.3390/molecules24081639>
PMID:[31027298](https://pubmed.ncbi.nlm.nih.gov/31027298/)
 20. Rajamani A, Borkowski K, Akre S, Fernandez A, Newman JW, Simon SI, Passerini AG. Oxylipins in triglyceride-rich lipoproteins of dyslipidemic subjects promote endothelial inflammation following a high fat meal. *Sci Rep.* 2019; 9:8655.
<https://doi.org/10.1038/s41598-019-45005-5>
PMID:[31209255](https://pubmed.ncbi.nlm.nih.gov/31209255/)
 21. Ramsden CE, Ringel A, Majchrzak-Hong SF, Yang J, Blanchard H, Zamora D, Loewke JD, Rapoport SI, Hibbeln JR, Davis JM, Hammock BD, Taha AY. Dietary linoleic acid-induced alterations in pro- and anti-nociceptive lipid autacoids: implications for idiopathic pain syndromes? *Mol Pain.* 2016; 12:1744806916636386.
<https://doi.org/10.1177/1744806916636386>
PMID:[27030719](https://pubmed.ncbi.nlm.nih.gov/27030719/)
 22. Caligiuri SP, Parikh M, Stamenkovic A, Pierce GN, Aukema HM. Dietary modulation of oxylipins in cardiovascular disease and aging. *Am J Physiol Heart Circ Physiol.* 2017; 313:H903–18.
<https://doi.org/10.1152/ajpheart.00201.2017>
PMID:[28801523](https://pubmed.ncbi.nlm.nih.gov/28801523/)
 23. Dexter DT, Carter CJ, Wells FR, Javoy-Agid F, Agid Y, Lees A, Jenner P, Marsden CD. Basal lipid peroxidation in substantia nigra is increased in Parkinson's disease. *J Neurochem.* 1989; 52:381–89.
<https://doi.org/10.1111/j.1471-4159.1989.tb09133.x>
PMID:[2911023](https://pubmed.ncbi.nlm.nih.gov/2911023/)
 24. De Franceschi G, Fecchio C, Sharon R, Schapira AH, Proukakis C, Bellotti V, de Laureto PP. A-synuclein structural features inhibit harmful polyunsaturated fatty acid oxidation, suggesting roles in neuroprotection. *J Biol Chem.* 2017; 292:6927–37.
<https://doi.org/10.1074/jbc.M116.765149>
PMID:[28232489](https://pubmed.ncbi.nlm.nih.gov/28232489/)
 25. Lee HJ, Bazinet RP, Rapoport SI, Bhattacharjee AK. Brain arachidonic acid cascade enzymes are upregulated in a rat model of unilateral Parkinson disease. *Neurochem Res.* 2010; 35:613–19.
<https://doi.org/10.1007/s11064-009-0106-6>
PMID:[19997776](https://pubmed.ncbi.nlm.nih.gov/19997776/)
 26. Vivekanantham S, Shah S, Dewji R, Dewji A, Khatri C, Ologunde R. Neuroinflammation in Parkinson's disease: role in neurodegeneration and tissue repair. *Int J Neurosci.* 2015; 125:717–25.
<https://doi.org/10.3109/00207454.2014.982795>
PMID:[25364880](https://pubmed.ncbi.nlm.nih.gov/25364880/)
 27. Refolo V, Stefanova N. Neuroinflammation and Glial Phenotypic Changes in Alpha-Synucleinopathies. *Front Cell Neurosci.* 2019; 13:263.
<https://doi.org/10.3389/fncel.2019.00263>
PMID:[31263402](https://pubmed.ncbi.nlm.nih.gov/31263402/)
 28. Guzman-Martinez L, Maccioni RB, Andrade V, Navarrete LP, Pastor MG, Ramos-Escobar N. Neuroinflammation as a common feature of neurodegenerative disorders. *Front Pharmacol.* 2019; 10:1008.
<https://doi.org/10.3389/fphar.2019.01008>
PMID:[31572186](https://pubmed.ncbi.nlm.nih.gov/31572186/)
 29. Haque ME, Akther M, Jakaria M, Kim IS, Azam S, Choi DK. Targeting the microglial NLRP3 inflammasome and its role in Parkinson's disease. *Mov Disord.* 2020; 35:20–33.
<https://doi.org/10.1002/mds.27874> PMID:[31680318](https://pubmed.ncbi.nlm.nih.gov/31680318/)
 30. Leitner GR, Wenzel TJ, Marshall N, Gates EJ, Klegeris A. Targeting toll-like receptor 4 to modulate neuroinflammation in central nervous system disorders. *Expert Opin Ther Targets.* 2019; 23:865–82.
<https://doi.org/10.1080/14728222.2019.1676416>
PMID:[31580163](https://pubmed.ncbi.nlm.nih.gov/31580163/)
 31. Mattson MP, Arumugam TV. Hallmarks of brain aging: adaptive and pathological modification by metabolic states. *Cell Metab.* 2018; 27:1176–99.
<https://doi.org/10.1016/j.cmet.2018.05.011>
PMID:[29874566](https://pubmed.ncbi.nlm.nih.gov/29874566/)
 32. Newcombe EA, Camats-Perna J, Silva ML, Valmas N, Huat TJ, Medeiros R. Inflammation: the link between comorbidities, genetics, and Alzheimer's disease. *J Neuroinflammation.* 2018; 15:276.
<https://doi.org/10.1186/s12974-018-1313-3>
PMID:[30249283](https://pubmed.ncbi.nlm.nih.gov/30249283/)
 33. Mounsey RB, Mustafa S, Robinson L, Ross RA, Riedel G, Pertwee RG, Teismann P. Increasing levels of the

- endocannabinoid 2-AG is neuroprotective in the 1-methyl-4-phenyl-1,2,3,6-tetrahydropyridine mouse model of Parkinson's disease. *Exp Neurol*. 2015; 273:36–44.
<https://doi.org/10.1016/j.expneurol.2015.07.024>
PMID:[26244281](https://pubmed.ncbi.nlm.nih.gov/26244281/)
34. Balgoma D, Checa A, Sar DG, Snowden S, Wheelock CE. Quantitative metabolic profiling of lipid mediators. *Mol Nutr Food Res*. 2013; 57:1359–77.
<https://doi.org/10.1002/mnfr.201200840>
PMID:[23828856](https://pubmed.ncbi.nlm.nih.gov/23828856/)
 35. Pochard C, Leclair-Visonneau L, Coron E, Neunlist M, Rolli-Derkinderen M, Derkinderen P. Cyclooxygenase 2 is upregulated in the gastrointestinal tract in Parkinson's disease. *Mov Disord*. 2018; 33:493–94.
<https://doi.org/10.1002/mds.27237> PMID:[29150878](https://pubmed.ncbi.nlm.nih.gov/29150878/)
 36. Blesa J, Trigo-Damas I, Dileone M, Del Rey NL, Hernandez LF, Obeso JA. Compensatory mechanisms in Parkinson's disease: circuits adaptations and role in disease modification. *Exp Neurol*. 2017; 298:148–61.
<https://doi.org/10.1016/j.expneurol.2017.10.002>
PMID:[28987461](https://pubmed.ncbi.nlm.nih.gov/28987461/)
 37. Mirdamadi JL. Cerebellar Role in Parkinson's Disease. *J Neurophysiol*. 2016; 116:917–919.
<https://doi.org/10.1152/jn.01132.2015>
PMID:[26792889](https://pubmed.ncbi.nlm.nih.gov/26792889/)
 38. Kaut O, Kuchelmeister K, Moehl C, Wüllner U. 5-methylcytosine and 5-hydroxymethylcytosine in brains of patients with multiple system atrophy and patients with Parkinson's disease. *J Chem Neuroanat*. 2019; 96:41–48.
<https://doi.org/10.1016/j.jchemneu.2018.12.005>
PMID:[30557654](https://pubmed.ncbi.nlm.nih.gov/30557654/)
 39. Newman LE, Shadel GS. Pink1/parkin link inflammation, mitochondrial stress, and neurodegeneration. *J Cell Biol*. 2018; 217:3327–29.
<https://doi.org/10.1083/jcb.201808118>
PMID:[30154188](https://pubmed.ncbi.nlm.nih.gov/30154188/)
 40. Stojkowska I, Wagner BM, Morrison BE. Parkinson's disease and enhanced inflammatory response. *Exp Biol Med (Maywood)*. 2015; 240:1387–95.
<https://doi.org/10.1177/1535370215576313>
PMID:[25769314](https://pubmed.ncbi.nlm.nih.gov/25769314/)
 41. Krashia P, Cordella A, Nobili A, La Barbera L, Federici M, Leuti A, Campanelli F, Natale G, Marino G, Calabrese V, Vedele F, Ghiglieri V, Picconi B, et al. Author correction: blunting neuroinflammation with resolvin D1 prevents early pathology in a rat model of Parkinson's disease. *Nat Commun*. 2019; 10:4725.
<https://doi.org/10.1038/s41467-019-12538-2>
PMID:[31611555](https://pubmed.ncbi.nlm.nih.gov/31611555/)
 42. Picillo M, Nicoletti A, Fetoni V, Garavaglia B, Barone P, Pellecchia MT. The relevance of gender in Parkinson's disease: a review. *J Neurol*. 2017; 264:1583–607.
<https://doi.org/10.1007/s00415-016-8384-9>
PMID:[28054129](https://pubmed.ncbi.nlm.nih.gov/28054129/)
 43. Weiduschat N, Mao X, Beal MF, Nirenberg MJ, Shungu DC, Henschcliff C. Sex differences in cerebral energy metabolism in Parkinson's disease: a phosphorus magnetic resonance spectroscopic imaging study. *Parkinsonism Relat Disord*. 2014; 20:545–48.
<https://doi.org/10.1016/j.parkreldis.2014.02.003>
PMID:[24593902](https://pubmed.ncbi.nlm.nih.gov/24593902/)
 44. Caranci G, Piscopo P, Rivabene R, Traficante A, Rizzo B, Castellano AE, Ruggieri S, Vanacore N, Confaloni A. Gender differences in Parkinson's disease: focus on plasma α -synuclein. *J Neural Transm (Vienna)*. 2013; 120:1209–15.
<https://doi.org/10.1007/s00702-013-0972-6>
PMID:[23328951](https://pubmed.ncbi.nlm.nih.gov/23328951/)
 45. McCarthy MM, Nugent BM, Lenz KM. Neuroimmunology and neuroepigenetics in the establishment of sex differences in the brain. *Nat Rev Neurosci*. 2017; 18:471–84.
<https://doi.org/10.1038/nrn.2017.61>
PMID:[28638119](https://pubmed.ncbi.nlm.nih.gov/28638119/)
 46. Goodfellow PN, Lovell-Badge R. SRY and sex determination in mammals. *Annu Rev Genet*. 1993; 27:71–92.
<https://doi.org/10.1146/annurev.ge.27.120193.000443>
PMID:[8122913](https://pubmed.ncbi.nlm.nih.gov/8122913/)
 47. Dewing P, Chiang CW, Sinchak K, Sim H, Fernagut PO, Kelly S, Chesselet MF, Micevych PE, Albrecht KH, Harley VR, Vilain E. Direct regulation of adult brain function by the male-specific factor SRY. *Curr Biol*. 2006; 16:415–20.
<https://doi.org/10.1016/j.cub.2006.01.017>
PMID:[16488877](https://pubmed.ncbi.nlm.nih.gov/16488877/)
 48. Lee J, Pinares-Garcia P, Loke H, Ham S, Vilain E, Harley VR. Sex-specific neuroprotection by inhibition of the y-chromosome gene, SRY, in experimental Parkinson's disease. *Proc Natl Acad Sci USA*. 2019; 116:16577–82.
<https://doi.org/10.1073/pnas.1900406116>
PMID:[31371505](https://pubmed.ncbi.nlm.nih.gov/31371505/)
 49. Chen W, Yan X, Lv H, Liu Y, He Z, Luo X. Gender differences in prevalence of LRRK2-associated Parkinson disease: a meta-analysis of observational studies. *Neurosci Lett*. 2020; 715:134609.
<https://doi.org/10.1016/j.neulet.2019.134609>
PMID:[31698024](https://pubmed.ncbi.nlm.nih.gov/31698024/)
 50. Erickson MA, Liang WS, Fernandez EG, Bullock KM, Thysell JA, Banks WA. Genetics and sex influence peripheral and central innate immune responses and blood-brain barrier integrity. *PLoS One*. 2018;

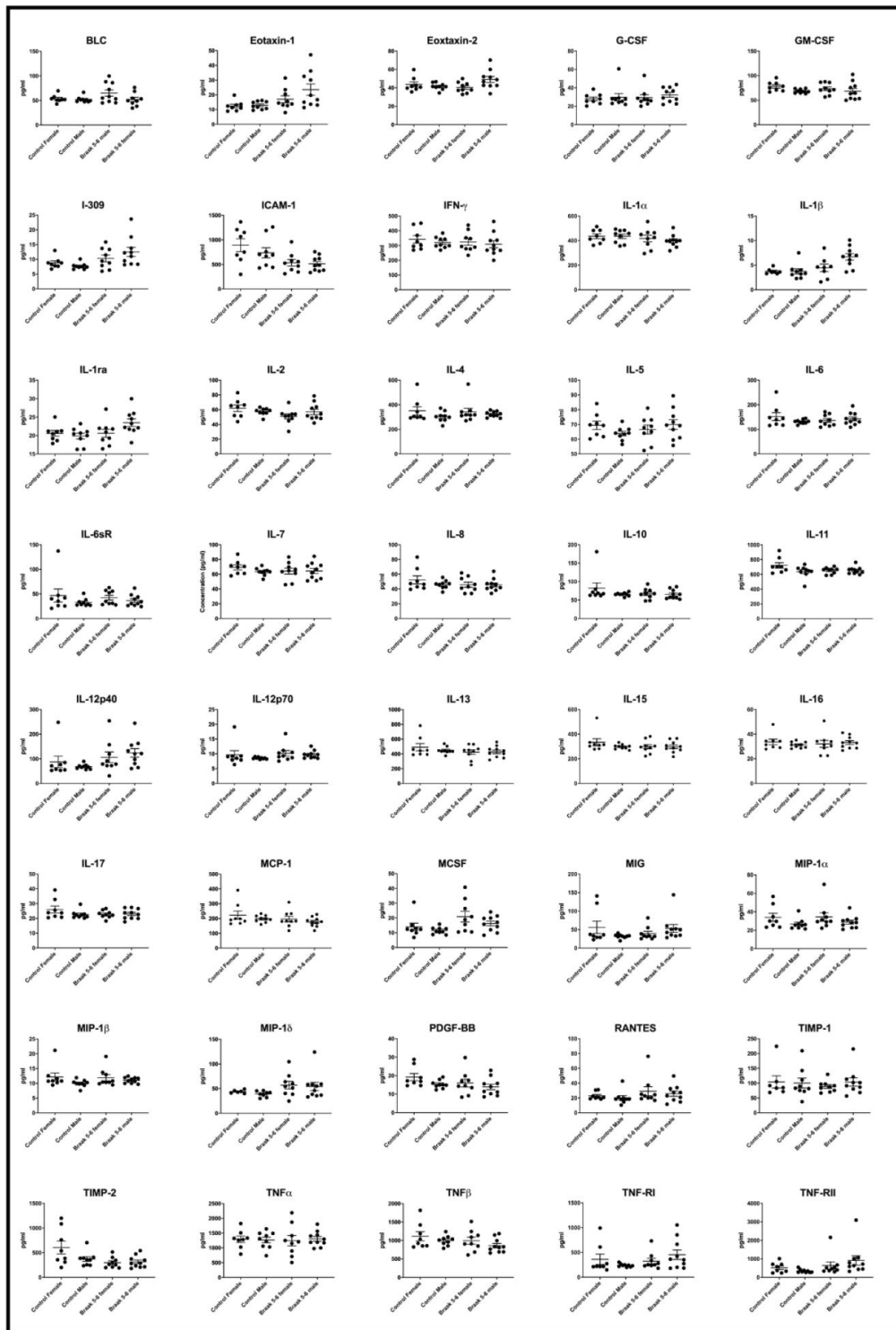
- 13:e0205769.
<https://doi.org/10.1371/journal.pone.0205769>
PMID:[30325961](https://pubmed.ncbi.nlm.nih.gov/30325961/)
51. Ferdouse A, Leng S, Winter T, Aukema HM. The brain oxylipin profile is resistant to modulation by dietary n-6 and n-3 polyunsaturated fatty acids in male and female rats. *Lipids*. 2019; 54:67–80.
<https://doi.org/10.1002/lipd.12122>
PMID:[30697757](https://pubmed.ncbi.nlm.nih.gov/30697757/)
52. Pace S, Sautebin L, Werz O. Sex-biased eicosanoid biology: impact for sex differences in inflammation and consequences for pharmacotherapy. *Biochem Pharmacol*. 2017; 145:1–11.
<https://doi.org/10.1016/j.bcp.2017.06.128>
PMID:[28647490](https://pubmed.ncbi.nlm.nih.gov/28647490/)
53. Giuliani N, Sansoni P, Girasole G, Vescovini R, Passeri G, Passeri M, Pedrazzoni M. Serum interleukin-6, soluble interleukin-6 receptor and soluble gp130 exhibit different patterns of age- and menopause-related changes. *Exp Gerontol*. 2001; 36:547–57.
[https://doi.org/10.1016/s0531-5565\(00\)00220-5](https://doi.org/10.1016/s0531-5565(00)00220-5)
PMID:[11250125](https://pubmed.ncbi.nlm.nih.gov/11250125/)
54. Scotland RS, Stables MJ, Madalli S, Watson P, Gilroy DW. Sex differences in resident immune cell phenotype underlie more efficient acute inflammatory responses in female mice. *Blood*. 2011; 118:5918–27.
<https://doi.org/10.1182/blood-2011-03-340281>
PMID:[21911834](https://pubmed.ncbi.nlm.nih.gov/21911834/)
55. Marriott I, Huet-Hudson YM. Sexual dimorphism in innate immune responses to infectious organisms. *Immunol Res*. 2006; 34:177–92.
<https://doi.org/10.1385/IR:34:3:177> PMID:[16891670](https://pubmed.ncbi.nlm.nih.gov/16891670/)
56. Chandra G, Rangasamy SB, Roy A, Kordower JH, Pahan K. Neutralization of RANTES and eotaxin prevents the loss of dopaminergic neurons in a mouse model of Parkinson disease. *J Biol Chem*. 2016; 291:15267–81.
<https://doi.org/10.1074/jbc.M116.714824>
PMID:[27226559](https://pubmed.ncbi.nlm.nih.gov/27226559/)
57. Lucas SM, Rothwell NJ, Gibson RM. The role of inflammation in CNS injury and disease. *Br J Pharmacol*. 2006 (Suppl 1); 147:S232–40.
<https://doi.org/10.1038/sj.bjp.0706400>
PMID:[16402109](https://pubmed.ncbi.nlm.nih.gov/16402109/)
58. Eikelenboom P, van Exel E, Hoozemans JJ, Veerhuis R, Rozemuller AJ, van Gool WA. Neuroinflammation - an early event in both the history and pathogenesis of Alzheimer's disease. *Neurodegener Dis*. 2010; 7:38–41.
<https://doi.org/10.1159/000283480>
PMID:[20160456](https://pubmed.ncbi.nlm.nih.gov/20160456/)
59. Kang KH, Liou HH, Hour MJ, Liou HC, Fu WM. Protection of dopaminergic neurons by 5-lipoxygenase inhibitor. *Neuropharmacology*. 2013; 73:380–87.
<https://doi.org/10.1016/j.neuropharm.2013.06.014>
PMID:[23800665](https://pubmed.ncbi.nlm.nih.gov/23800665/)
60. Fischer R, Maier O, Siegemund M, Wajant H, Scheurich P, Pfizenmaier K. A TNF receptor 2 selective agonist rescues human neurons from oxidative stress-induced cell death. *PLoS One*. 2011; 6:e27621.
<https://doi.org/10.1371/journal.pone.0027621>
PMID:[22110694](https://pubmed.ncbi.nlm.nih.gov/22110694/)
61. Garwood CJ, Cooper JD, Hanger DP, Noble W. Anti-inflammatory impact of minocycline in a mouse model of tauopathy. *Front Psychiatry*. 2010; 1:136.
<https://doi.org/10.3389/fpsy.2010.00136>
PMID:[21423446](https://pubmed.ncbi.nlm.nih.gov/21423446/)
62. Alafuzoff I, Ince PG, Arzberger T, Al-Sarraj S, Bell J, Bodi I, Bogdanovic N, Bugiani O, Ferrer I, Gelpi E, Gentleman S, Giaccone G, Ironside JW, et al. Staging/typing of lewy body related alpha-synuclein pathology: a study of the BrainNet europe consortium. *Acta Neuropathol*. 2009; 117:635–52.
<https://doi.org/10.1007/s00401-009-0523-2>
PMID:[19330340](https://pubmed.ncbi.nlm.nih.gov/19330340/)
63. Shephard F, Greville-Heygate O, Marsh O, Anderson S, Chakrabarti L. A mitochondrial location for haemoglobins—dynamic distribution in ageing and Parkinson's disease. *Mitochondrion*. 2014; 14:64–72.
<https://doi.org/10.1016/j.mito.2013.12.001>
PMID:[24333691](https://pubmed.ncbi.nlm.nih.gov/24333691/)
64. Sigma-Aldrich. Technical bulletin: Bradford Reagent B6916.
<https://www.sigmaaldrich.com/content/dam/sigma-aldrich/docs/Sigma/Bulletin/b6916bul.pdf>
65. Shephard F, Greville-Heygate O, Liddell S, Emes R, Chakrabarti L. Analysis of mitochondrial haemoglobin in Parkinson's disease brain. *Mitochondrion*. 2016; 29:45–52.
<https://doi.org/10.1016/j.mito.2016.05.001>
PMID:[27181046](https://pubmed.ncbi.nlm.nih.gov/27181046/)
66. Richardson D, Ortori CA, Chapman V, Kendall DA, Barrett DA. Quantitative profiling of endocannabinoids and related compounds in rat brain using liquid chromatography-tandem electrospray ionization mass spectrometry. *Anal Biochem*. 2007; 360:216–26.
<https://doi.org/10.1016/j.ab.2006.10.039>
PMID:[17141174](https://pubmed.ncbi.nlm.nih.gov/17141174/)

SUPPLEMENTARY MATERIALS

Supplementary Figures



Supplementary Figure 1. A large variation of oxylipin concentration is seen in the control female group. Comparison of measured oxylipins in cerebellar mitochondria from PD males (Braak 3-4 and 5-6) and PD females (Braak 5-6) and age-matched controls. PD Braak 3-4 male n=5; PD Braak 5-6 male n=5; PD Braak 5-6 female n=5; control male n=5; control female n=5. Plots display mean quantities (pmol/g) ± SEM. For *p* and *f* values refer to Supplementary Tables 3 and 4.



Supplementary Figure 2. Graphical comparisons of all measured inflammatory cytokines from cerebellar mitochondria of males and females with Braak stage 5-6 Parkinson’s disease and age-matched controls. PD Braak 5-6 male n=10; PD Braak 5-6 female n=9; control male n=9; control female n=8. Plots display mean concentration (pg/ml) ± SEM. For all *p* or *f* values refer to Supplementary Tables 5 or 6, respectively.

Supplementary Tables

Supplementary Table 1. Human post-mortem samples information.

ID	Diagnosis	Age (yr)	Sex	Disease duration (yr)	α -syn	Cause of death	Post mortem delay (hr)
75/02	Control	61	F	N/A	N/A	Not reported	N/A
CO48	Control	68	M	N/A	N/A	Metastatic colon cancer	10
CO22	Control	69	F	N/A	N/A	Lung cancer	33
PDC008	Control	71	F	N/A	N/A	Myocardial infarction	17
PDC030	Control	77	M	N/A	N/A	Conductive cardiac failure	17
CO45	Control	77	M	N/A	N/A	Multiple (old age)	22
CO26	Control	78	F	N/A	N/A	Myeloid leukaemia	33
61/07	Control	81	M	N/A	N/A	Not reported	N/A
PDC029	Control	82	M	N/A	N/A	Metastatic liver/lung cancer	48
PDC005	Control	58	M	N/A	N/A	Not reported	9
PDC022	Control	65	M	N/A	N/A	Lung carcinoma	12
PDC034	Control	90	M	N/A	N/A	Respiratory failure	12
PDC016	Control	93	F	N/A	N/A	Bronchial pneumonia/old	22
PDC026	Control	80	F	N/A	N/A	Breast carcinoma	23
PDC023	Control	78	F	N/A	N/A	Not reported	23
PDC008	Control	71	F	N/A	N/A	Myocardial infarction	17
PDC028	Control	84	F	N/A	N/A	Pancreatic cancer	11
PDC027	Control	79	M	N/A	N/A	Cardiac arrest & pneumonia	21
PDC092	Control	79	M	N/A	N/A	Brainstem stroke, bronchopneumonia	25
PDC014	Control	64	M	N/A	N/A	Cardiac failure	18
PDC078	Control	91	M	N/A	N/A	Not reported	18
PDC105	Control	95	M	N/A	N/A	Pneumonia, cellulitis of leg	11
PDC053	Control	89	F	N/A	N/A	Not reported	22
PDC040	Control	61	F	N/A	N/A	Ovarian cancer	15
PD081	Braak 3-4	73	M	9	6	Not reported	19
PD036	Braak 3-4	76	M	10	3	Not reported	10
PD041	Braak 3-4	77	M	10	6	Not reported	6
PD007	Braak 3-4	78	M	10	3	Pneumonia	22
PD067	Braak 3-4	83	M	9	6	Not reported	10
PD051	Braak 3-4	80	M	5	5	Not reported	7
PD067	Braak 3-4	83	M	9	N/A	Not reported	10
PD081	Braak 3-4	73	M	9	N/A	Not reported	19
PD084	Braak 3-4	78	M	9	5	Ischaemic bowel and atrial fibrillation	3
PD074	Braak 3-4	85	M	5	5	bronchopneumonia	7
002/08	Braak 5-6	69	M	1	Not available	Not reported	N/A
PD131	Braak 5-6	76	F	11	6	Not reported	22
044/07	Braak 5-6	78	M	6	Not available	Not reported	N/A
PD014	Braak 5-6	79	M	12	3	Parkinson's	21
PD063	Braak 5-6	80	F	13	4	Old age and PD	10
PD028	Braak 5-6	82	M	18	6	Not reported	14
PD050	Braak 5-6	82	F	14	6	Chest infection & CVA	18
PD099	Braak 5-6	82	M	11	6	Pneumonia	10
PD016	Braak 5-6	85	F	18	6	Bronchopneumonia/PD	14
PD045	Braak 5-6	80	M	19	6	Not reported	16
PD028	Braak 5-6	82	M	18	6	Not reported	14
PD079	Braak 5-6	78	F	19	6	Chest infection & CVA	22
PD016	Braak 5-6	85	F	18	6	Bronchopneumonia/PD	14
PD125	Braak 5-6	74	M	25	6	Bronchopneumonia/PD	20
PD117	Braak 5-6	77	F	31	5	Not reported	6
PD021	Braak 5-6	76	M	27	6	Not reported	17
PD020	Braak 5-6	75	M	34	6	Not reported	2

PD117	Braak 5-6	77	F	31	5	Not reported	6
PD017	Braak 5-6	75	M	18	6	Not reported	22
PD180	Braak 5-6	85	F	15	6	Chest infection & PD	15
PD093	Braak 5-6	81	F	14	6	Not reported	22
PD203	Braak 5-6	84	F	18	6	PD	19
PD413	Braak 5-6	72	F	21	6	Pneumonia	14

Supplementary Table 2. Abbreviations and corresponding full names of all oxylipins, inflammatory cytokines and endocannabinoids used in this work.

Abbreviation	
<i>Oxylipins</i>	
AA	Arachidonic acid
LA	Linoleic acid
12-HETE	12-hydroxyeicosatetraenoic acid
TXB-2	Thromboxane B2
PGE2	Prostaglandin E ₂
5-HETE	5-Hydroxyeicosatetraenoic acid
5-HPETE	Arachidonic acid 5-hydroperoxide
12-HPETE	Arachidonic acid 12-hydroperoxide
9-HETE	9-Hydroxyeicosatetraenoic acid
20-HETE	20-Hydroxyeicosatetraenoic acid
LTB-4	Leukotriene B4
9-oxoODE	9-oxo-10E,12Z-octadecadienoic acid
9-HODE	9S-Hydroxy-10E,12Z-octadecadienoic acid
5,6-EET	5,6-epoxyeicosatrienoic acid
5,6-DHET	5,6-dihydroxyeicosatrienoic acid
8,9-DHET	8,9-dihydroxyeicosatrienoic acid
11,12-DHET	11,12-dihydroxyeicosatrienoic acid
14,15-DHET	14,15-dihydroxyeicosatrienoic acid
8-HETE	8-Hydroxyeicosatetraenoic acid
11-HETE	11-Hydroxyeicosatetraenoic acid
15-HETE	15-Hydroxyeicosatetraenoic acid
16-HETE	16-Hydroxyeicosatetraenoic acid
8,9-EET	8,9-epoxyeicosatrienoic acid
11,12-EET	11,12-epoxyeicosatrienoic acid
14,15-EET	14,15-epoxyeicosatrienoic acid
17-HDoHE	17-Hydroxydocosahexaenoic acid
13-oxoODE	13-Oxo-9,11-octadecadienoic acid
13-HODE	13-hydroxy-9Z,11E-octadecadienoic acid
8,15-DiHETE	8,15-Leukotriene B4
<i>Endocannabinoids</i>	
2-AG	2-Arachidonoylglycerol
AEA	Anandamide
OEA	Oleyethanolamide
PEA	Palmitoylethanolamide
<i>Inflammatory cytokines</i>	
BLC	B Cell-Attracting Chemokine 1
Eotaxin	C-C Motif Chemokine Ligand 11 (CCL11)
Eotaxin-2	C-C Motif Chemokine Ligand 24 (CCL24)
G-CSF	Granulocyte Colony-Stimulating Factor
GM-CSF	Granulocyte-Macrophage Colony-Stimulating Factor

I-309	C-C Motif Chemokine Ligand 1 (CCL1)
ICAM-1	Intercellular Adhesion Molecule 1
IFN γ	Interferon Gamma
IL-1 α	Interleukin 1 Alpha
IL-1 β	Interleukin 1 Beta
IL-2	Interleukin 2
IL-6	Interleukin 6
IL-6sR	Interleukin 6 soluble receptor
IL-7	Interleukin 7
IL-8	Interleukin 8
IL-12p40	IL-12 Subunit P40
IL-12p70	IL-12 Subunit P70
IL-15	Interleukin 15
IL-16	Interleukin 16
IL-17	Interleukin 17
MCP-1	Monocyte Chemotactic And Activating Factor
MIG	Monokine Induced By Interferon-Gamma
MIP-1 α	Macrophage Inflammatory Protein 1-Alpha
MIP-1 β	Macrophage Inflammatory Protein 1-Beta
MIP-1 δ	Macrophage Inflammatory Protein 1-Delta
PDGF-BB	Platelet Derived Growth Factor Subunit B
RANTES	Regulated Upon Activation, Normally T-Expressed, And Secreted
TNF α	Tumor Necrosis Factor-Alpha
TNF β	Tumor Necrosis Factor-Beta
TNF RI	Tumor Necrosis Factor Receptor 1
TNF RII	Tumor Necrosis Factor Receptor 2
IL-1ra	Interleukin 1 Receptor Antagonist
IL-4	Interleukin 4
IL-5	Interleukin 5
IL-10	Interleukin 10
IL-11	Interleukin 11
IL-13	Interleukin 13
MCSF	Macrophage Colony-Stimulating Factor 1
TIMP-1	Tissue Inhibitor Of Metalloproteinases 1
TIMP-2	Tissue Inhibitor Of Metalloproteinases 2

Supplementary Table 3. Mean comparisons of all 29 measured oxylipins from cerebellar mitochondria.

Oxylipin	Control males vs control females	Braak 5-6 males vs Braak 5-6 females	Braak 5-6 males vs control males	Braak 3-4 males vs control males	Braak 3-4 males vs Braak 5-6 males	Braak 3-4 males vs control females	Braak 5-6 females vs control females
AA	0.4206	0.1429	>0.9999	>0.9999	0.688	0.6905	0.0317*
LA	0.4206	0.1984	>0.9999	>0.9999	>0.9999	0.6905	0.0556
12-HETE	0.0079**	0.5159	0.5373	0.1209	>0.9999	0.2222	0.0317*
TXB-2	0.0556	0.8571	>0.9999	0.1687	0.0589	0.5476	0.0317*
PGE2	0.2222	0.6032	>0.9999	0.198	0.7737	>0.9999	0.2778
5-HETE	0.2222	0.3968	>0.9999	0.1687	0.6093	0.6905	0.0476*
5-HPETE	0.0952	0.381	>0.9999	>0.9999	0.8665	0.5476	0.0317*
12-HPETE	0.3095	0.6508	0.6905	0.3095	0.5476	0.5476	0.0476*
9-HETE	0.2222	0.8016	>0.9999	0.1431	0.3116	0.5476	0.0873
20-HETE	0.2222	0.5238	>0.9999	0.4127	0.6093	0.8413	0.0873
LTB-4	0.4206	0.7857	>0.9999	0.1204	0.0139*	0.6905	0.2063
9-oxoODE	0.3095	0.1905	>0.9999	>0.9999	>0.9999	0.4206	0.0476*
9-HODE	0.2222	0.1905	>0.9999	0.3339	0.0774	0.6905	0.0476*
5,6-EET	0.1508	0.381	>0.9999	0.4719	>0.9999	0.8413	0.0317*
5,6-DHET	0.3095	0.5238	0.6081	0.1311	>0.9999	0.5476	0.381
8,9-DHET	0.2222	0.5397	>0.9999	0.5373	>0.9999	0.3095	0.2063
11,12-DHET	0.2222	0.3968	>0.9999	0.3116	0.7737	0.5476	0.1349
14,15-DHET	0.3095	0.5159	>0.9999	0.2691	0.6093	0.4206	0.1984
8-HETE	0.2222	0.381	>0.9999	0.0589	0.2691	0.6905	0.0873
11-HETE	0.2222	0.5	>0.9999	0.1687	0.1017	0.8413	0.1349
15-HETE	0.1508	0.5238	>0.9999	0.3116	0.3594	0.6905	0.0873
16-HETE	0.3095	0.3968	>0.9999	0.2313	0.198	0.8413	0.0476*
8,9-EET	0.2222	0.2778	>0.9999	0.071	0.3594	0.6905	0.0873
11,12-EET	0.2222	0.5159	>0.9999	0.198	0.0851	0.6905	0.1984
14,15-EET	0.1508	0.5238	>0.9999	0.4127	0.6093	0.6905	0.0873
17-HDoHE	0.2222	0.381	>0.9999	>0.9999	>0.9999	0.6905	0.0476*
13-oxoODE	0.2222	0.2857	>0.9999	>0.9999	>0.9999	0.3095	0.0476*
13-HODE	0.2222	0.1905	>0.9999	0.2691	0.1017	0.5476	0.0476*
8,15-DiHETE	>0.9999	0.5238	>0.9999	0.5338	>0.9999	0.0952	0.8968

PD Braak 3-4 male n=5; PD Braak 5-6 male n=5; PD Braak 5-6 female n=5; control male n=5; control female n=5. Statistical analyses were carried out using GraphPad Prism (Kruskal-Wallis test with multiple comparisons or Mann-Whitney U-test where appropriate). Red and blue font oxylipins represent pro- and anti-inflammatory, respectively. Bright yellow shaded numbers refer to significance (* p <0.05; ** p <0.01).

Supplementary Table 4. Group variance analyses of all 29 measured oxylipins from cerebellar mitochondria.

Oxylipin	Control males vs control females	Braak 5-6 males vs Braak 5-6 females	Braak 5-6 males vs control males	Braak 3-4 males vs control males	Braak 3-4 males vs Braak 5-6 males	Braak 3-4 males vs control females	Braak 5-6 females vs control females
AA	0.001**	0.9319	0.0209*	0.0072**	0.5974	0.3514	0.1354
LA	0.0048**	0.3855	0.4618	0.9381	0.4176	0.0041**	0.0036**
12-HETE	0.4458	0.9151	0.2903	0.453	0.7467	0.9901	0.8379
TXB-2	0.5039	0.903	0.6142	0.2706	0.5359	0.0895	0.2078
PGE2	0.0517	0.125	0.4369	0.349	0.8676	0.2616	0.0104*
5-HETE	0.0402*	0.2352	0.2075	0.3246	0.7657	0.2306	0.0468*
5-HPETE	0.1729	0.0686	0.538	0.6102	0.2696	0.0715	0.0149*
12-HPETE	0.3939	0.0208*	0.9326	0.2237	0.1959	0.0503	0.0043**
9-HETE	0.0878	0.8281	0.948	0.3884	0.3553	0.3558	0.1145
20-HETE	0.0641	0.9358	0.5881	0.2454	0.5188	0.4326	0.1447
LTB-4	0.0567	0.454	0.7851	0.3996	0.5632	0.0108*	0.1338
9-oxoODE	0.0173*	0.2025	0.8634	0.2913	0.3717	0.0019**	0.0008***
9-HODE	0.0272*	0.2072	0.7879	0.6756	0.8803	0.0119*	0.0011**
5,6-EET	0.1154	0.0308*	0.6494	0.5482	0.2996	0.0385*	0.0027**
5,6-DHET	0.1545	0.5922	0.4865	0.1216	0.3628	0.8868	0.8066
8,9-DHET	0.1304	0.1762	0.7949	0.6324	0.4639	0.28	0.6597
11,12-DHET	0.3047	0.158	0.8692	0.7037	0.5873	0.5078	0.0169
14,15-DHET	0.137	0.9187	0.8623	0.669	0.5498	0.2709	0.1214
8-HETE	0.0431*	0.8093	0.516	0.4253	0.8786	0.1791	0.2063
11-HETE	0.0707	0.8643	0.535	0.5844	0.9402	0.1819	0.2665
15-HETE	0.0759	0.8024	0.6538	0.5574	0.8881	0.2066	0.108
16-HETE	0.268	0.4558	0.9429	0.8615	0.9181	0.2051	0.0674
8,9-EET	0.0408*	0.8163	0.5151	0.3884	0.8263	0.1907	0.1947
11,12-EET	0.0946	0.7192	0.7711	0.5743	0.7844	0.2406	0.274
14,15-EET	0.0859	0.7794	0.675	0.5518	0.8582	0.2331	0.1098
17-HDoHE	0.0951	0.1531	0.9555	0.7221	0.764	0.174	0.006**
13-oxoODE	0.0085**	0.2321	0.7652	0.4311	0.2845	0.0016**	0.0012**
13-HODE	0.0138*	0.1104	0.7363	0.3799	0.5811	0.0022**	0.0002***
8,15-DiHETE	0.5978	0.1323	0.0999	0.5292	0.2795	0.9173	0.7143

PD Braak 3-4 male n=5; PD Braak 5-6 male n=5; PD Braak 5-6 female n=5; control male n=5; control female n=5. Statistical analyses were carried out using GraphPad Prism (*f*-test). Red and blue font oxylipins represent pro- and anti-inflammatory, respectively. Bright yellow shaded numbers refer to significance (**p*<0.05; ***p*<0.01; ****p*<0.001).

Supplementary Table 5. Statistical comparisons of all 40 measured inflammatory cytokines from cerebellar mitochondria.

Inflammatory Cytokine	Control males vs control females	Braak 5-6 males vs Braak 5-6 females	Braak 5-6 males vs control males	Braak 5-6 females vs control females
BLC	0.4807	0.1564	0.1823	0.5414
Eotaxin	0.6058	0.4363	0.04*	0.0745
Eotaxin-2	0.8884	0.077	0.0503	0.3704
G-CSF	0.8884	0.3562	0.3154	>0.9999
GM-CSF	0.0418*	0.4002	0.6607	>0.9999
I-309	0.0745	0.5457	0.0005***	0.4234
ICAM-1	0.4234	>0.9999	0.0789	0.0274*
IFNγ	0.8148	0.447	0.3562	0.6058
IL-1α	0.9626	0.447	0.2428	0.743
IL-1β	0.536	0.0545	0.0057**	0.3357
IL-2	0.3213	0.447	0.7197	0.1388
IL-6	0.4807	0.6607	0.549	0.5414
IL-6sR	0.743	0.3562	0.6038	0.5414
IL-7	0.3213	0.9048	0.9682	0.6058
IL-8	0.743	0.9048	0.549	0.3213
IL-12p40	0.8148	0.4894	0.0188*	0.1672
IL-15	0.2766	0.9048	0.8421	0.3213
IL-16	0.5414	0.8421	0.4967	0.6058
IL-17	0.2359	0.8421	0.9048	0.6058
MCP-1	0.8148	0.4002	0.1333	0.4807
MIG	0.4807	0.2581	0.0188*	0.8148
MIP-1α	0.1388	0.3154	0.3154	>0.9999
MIP-1β	0.0927	>0.9999	0.0653	0.8148
MIP-1δ	0.1812	0.4967	0.1728	0.2721
PDGF-BB	0.1139	0.6038	0.3154	0.2359
RANTES	0.007**	0.9682	0.1011	0.6058
TNFα	0.9626	0.6607	0.9048	0.5414
TNFβ	0.9626	0.3154	0.0789	0.6058
TNF RI	0.9626	0.4967	0.1564	0.3704
TNF RII	0.3213	0.2224	0.0012**	0.9626
IL-1ra	0.6058	0.0535	0.0057**	0.8884
IL-4	0.5414	0.9682	0.1823	0.8148
IL-5	0.2359	0.4967	0.1823	0.673
IL-10	0.4234	0.7802	0.6607	0.6058
IL-11	0.1672	0.9048	0.7802	0.1996
IL-12p70	0.743	>0.9999	0.0101*	0.3213
IL-13	0.673	0.9682	0.6607	0.8148
MCSF	0.743	0.4967	0.0653	0.1996
TIMP-1	0.9182	0.4967	0.6607	0.9182
TIMP-2	0.3704	0.7802	0.2428	0.036*

PD Braak 5-6 male n=10; PD Braak 5-6 female n=9; control male n=9; control female n=8. Statistical analyses were carried out using GraphPad Prism (Mann-Whitney U-test). Red and blue font represent pro- and anti-inflammatory, respectively. Bright yellow shaded numbers refer to significance (* p <0.05; ** p <0.01; *** p <0.001).

Supplementary Table 6. Statistical group variance analyses of all 40 measured inflammatory cytokines from cerebellar mitochondria.

Inflammatory Cytokine	Control males vs control females	Braak 5-6 males vs Braak 5-6 females	Braak 5-6 males vs control males	Braak 5-6 females vs control females
BLC	0.489	0.2784	0.0024**	0.1595
Eotaxin	0.4921	0.4269	0.0017**	0.0723
Eotaxin-2	0.0547	0.4614	0.0586	0.429
G-CSF	0.0785	0.5697	0.269	0.1925
GM-CSF	0.1593	0.2312	0.0004***	0.2614
I-309	0.114	0.7636	0.0054**	0.1258
ICAM-1	0.6282	0.4518	0.0546	0.1108
IFNγ	0.0864	0.7262	0.057	0.8382
IL-1α	0.9418	0.1935	0.8813	0.321
IL-1β	0.0221*	0.8982	0.4273	0.0042**
IL-2	0.0155*	0.7287	0.0202*	0.5979
IL-6	0.0001***	0.7721	0.0065**	0.0755
IL-6sR	0.0002***	0.5675	0.2664	0.0145*
IL-7	0.1184	0.8129	0.0419*	0.5199
IL-8	0.0117*	0.6105	0.2609	0.2745
IL-12p40	<0.0001****	0.129	0.0013**	0.9745
IL-15	0.0007***	0.728	0.0263*	0.2327
IL-16	0.0166*	0.1326	0.0653	0.4724
IL-17	0.0279*	0.3974	0.5947	0.0138*
MCP-1	0.0028**	0.1306	0.3733	0.3504
MIG	<0.0001****	0.1617	0.0902	0.0155*
MIP-1α	0.0575	0.0419*	0.7264	0.7378
MIP-1β	0.0044**	0.0023**	0.5406	0.5712
MIP-1δ	0.2335	0.732	0.0006***	0.0005***
PDGF-BB	0.0203*	0.4083	0.0396*	0.6927
RANTES	0.3007	0.1473	0.0046**	0.0026**
TNFα	0.8404	0.0413*	0.7458	0.1598
TNFβ	0.0155*	0.2411	0.3658	0.569
TNF RI	<0.0001****	0.1133	<0.0001****	0.1464
TNF RII	0.0079**	0.0696	0.0123*	0.0479*
IL-1ra	0.9013	0.998	0.362	0.3329
IL-4	0.0349*	0.0005***	0.0917	0.8174
IL-5	0.1335	0.7278	0.0301*	0.755
IL-10	<0.0001****	0.6593	0.0095**	0.0097**
IL-11	0.5622	0.7733	0.1148	0.024*
IL-12p70	<0.0001****	0.0408*	0.0004***	0.337
IL-13	0.0072**	0.5229	0.1929	0.3199
MCSF	0.0052**	0.0439*	0.0367*	0.3129
TIMP-1	0.793	0.0265*	0.7116	0.0087**
TIMP-2	0.0139*	0.7664	0.6342	0.0022**

PD Braak 5-6 male n=10; PD Braak 5-6 female n=9; control male n=9; control female n=8. Statistical analyses were carried out using GraphPad Prism (*f*-test). Red and blue font represent pro- and anti-inflammatory cytokines, respectively. Bright yellow shaded numbers refer to significance (**p*<0.05; ***p*<0.01; ****p*<0.001; *****p*<0.0001).

Supplementary Table 7. Statistical comparisons of endocannabinoids were carried out using GraphPad Prism (Kruskal-Wallis and *f* tests).

Endocannabinoid	Control males vs control females	Braak 5-6 males vs Braak 5-6 females	Braak 5-6 females vs control females	Braak 5-6 males vs control males
<i>p-values</i>				
2-AG	>0.9999	>0.9999	>0.9999	>0.9999
AEA	>0.9999	>0.9999	>0.9999	>0.9999
OEA	>0.9999	>0.9999	0.9232	>0.9999
PEA	>0.9999	>0.9999	>0.9999	>0.9999
<i>f-values</i>				
2-AG	0.1801	0.0441*	0.0336*	0.2331
AEA	0.0829	0.9996	0.0164*	0.5157
OEA	0.733	0.8458	0.6317	0.9572
PEA	0.7027	0.0814	0.0397*	0.9634

Bright yellow shaded numbers refer to significance (**p*<0.05). Braak 5-6 male n=8; Braak 5-6 female n=9; control male n=8; control female n=6. All samples were age matched.